

# Expression of the Transcriptional Repressor Protein Kid-1 Leads to the Disintegration of the Nucleolus\*

(Received for publication, December 12, 1997, and in revised form, November 20, 1998)

Zhiqing Huang<sup>‡</sup>, Bärbel Philippin<sup>‡</sup>, Eileen O'Leary<sup>§</sup>, Joseph V. Bonventre<sup>§¶</sup>, Wilhelm Kriz<sup>‡</sup>, and Ralph Witzgall<sup>‡¶</sup>

From the <sup>‡</sup>Institute of Anatomy and Cell Biology I, University of Heidelberg, Germany and the <sup>§</sup>Renal Unit, Massachusetts General Hospital and the <sup>¶</sup>Department of Medicine, Harvard Medical School, Charlestown, Massachusetts 02129

The rat *Kid-1* gene codes for a 66-kDa protein with KRAB domains at the NH<sub>2</sub> terminus and two Cys<sub>2</sub>His<sub>2</sub>-zinc finger clusters of four and nine zinc fingers at the COOH terminus. It was the first KRAB-zinc finger protein for which a transcriptional repressor activity was demonstrated. Subsequently, the KRAB-A domain was identified as a widespread transcriptional repressor motif. We now present a biochemical and functional analysis of the Kid-1 protein in transfected cells. The full-length Kid-1 protein is targeted to the nucleolus and adheres tightly to as yet undefined nucleolar structures, leading eventually to the disintegration of the nucleolus. The tight adherence and nucleolar distribution can be attributed to the larger zinc finger cluster, whereas the KRAB-A domain is responsible for the nucleolar fragmentation. Upon disintegration of the nucleolus, the nucleolar transcription factor upstream binding factor disappears from the nucleolar fragments. In the absence of Kid-1, the KRIP-1 protein, which represents the natural interacting partner of zinc finger proteins with a KRAB-A domain, is homogeneously distributed in the nucleus, whereas coexpression of Kid-1 leads to a shift of KRIP-1 into the nucleolus. Nucleolar run-ons demonstrate that rDNA transcription is shut off in the nucleolar fragments. Our data demonstrate the functional diversity of the KRAB and zinc finger domains of Kid-1 and provide new functional insights into the regulation of the nucleolar structure.

Transcriptional repression is increasingly recognized as an important feature of genetic and epigenetic regulation (for recent reviews, see Refs. 1 and 2). While several proteins have been described as transcriptional repressors, the number of motifs conferring transcriptional repressor activity has so far been rather limited. A widespread transcriptional repressor motif is the KRAB-A domain (3–6), which is found in approximately one-third of all zinc finger proteins of the Cys<sub>2</sub>His<sub>2</sub> class (7, 8). Zinc finger proteins of the Cys<sub>2</sub>His<sub>2</sub> class represent one of the largest protein families known; the mammalian genome contains several hundred genes coding for such proteins (9), and the KRAB-A domain therefore represents a very

important paradigm of transcriptional repression. Experiments from several laboratories have shown that the KRAB-A domain represses transcription both upstream and downstream of a target gene and is able to do so from a distance (5, 10). In addition, the KRAB-A domain has to be tethered to DNA via fusion to a DNA-binding domain in order to exert its repressor activity (3). This suggests that the KRAB-A domain interacts with other proteins and rules out other modes of action such as squelching or steric hindrance. Interestingly, the KRAB-A domain does not repress transcription in the context of any promoter, but only works in certain contexts. Fusion proteins with the KRAB-A domain repress RNA polymerase II promoters with a TATA box and an initiator element but not promoters with an initiator element only (11). It has also been reported that in addition to RNA polymerase II-mediated transcription, the KRAB-A domain also represses RNA polymerase III-mediated transcription, whereas transcription by RNA polymerase I and T7 RNA polymerase do not appear to be inhibited (10). By conventional biochemical techniques and the two-hybrid cloning protocol, a KRAB-A interacting protein called KAP-1 (12), TIF1 $\beta$  (13), and KRIP-1 (14) was cloned. The KRIP-1/KAP-1/TIF1 $\beta$  cDNA codes for a protein with a predicted relative molecular weight of 89 kDa and contains several characteristic modules that suggest that it is involved in remodeling chromatin, thus providing a hint to how the KRAB-A domain represses transcription.

The zinc finger protein Kid-1 was cloned as a result of a screen for transcription factors that are regulated after acute renal failure and during renal development (15). The Kid-1 protein (kidney, ischemia, development) contains 13 Cys<sub>2</sub>His<sub>2</sub>-zinc fingers at its COOH terminus and KRAB-A and -B domains at its NH<sub>2</sub> terminus; it was the first KRAB-zinc finger protein for which a transcriptional repressor activity could be demonstrated (15). By Northern blot and reverse transcription-polymerase chain reaction analysis, the Kid-1 mRNA is expressed predominantly in the adult rat kidney (15). In kidneys of newborn rats, when many nephrons are not fully developed, only low amounts of Kid-1 mRNA can be detected, whereas in the kidneys of adult rats the Kid-1 mRNA is expressed at its highest levels. During the recovery phase after ischemic acute tubular necrosis, Kid-1 mRNA levels are reduced transiently until the injured epithelium is restored (15). Kid-1 therefore possesses all of the hallmarks of a transcription factor that plays an important role in the regulation of an advanced stage of kidney development. We now present a careful analysis of the distribution of the Kid-1 protein demonstrating that expression of Kid-1 leads to the disruption of the nucleolus.

## MATERIALS AND METHODS

*Construction of Kid-1 Mutant Proteins*—The cDNA and cDNA fragments coding for the full-length and mutant Kid-1 proteins were cloned

\* This work was supported by the Deutsche Forschungsgemeinschaft Grants Wi 1042/2–1 and Wi 1042/2–2 (to R. W.) and National Institutes of Health Grant DK39773 (to J. V. B.). The costs of publication of this article were defrayed in part by the payment of page charges. This article must therefore be hereby marked "advertisement" in accordance with 18 U.S.C. Section 1734 solely to indicate this fact.

¶ To whom correspondence should be addressed: University of Heidelberg, Institute of Anatomy and Cell Biology I, Im Neuenheimer Feld 307, 69120 Heidelberg, Germany. Tel.: 49-6221-548686; Fax: 49-6221-544951; E-mail: ralph.witzgall@ur.z.uni-heidelberg.de.

into the mammalian expression vector pMT3. The pMT3 vector codes for fusion proteins with an epitope tag of the influenza virus hemagglutinin protein at the NH<sub>2</sub> terminus (HA<sup>1</sup> tag). Transcription is driven by the adenovirus major late promoter; in addition, pMT3 contains the SV40 origin of replication. Sequences of the fusion proteins are as follows (codons encoding the HA tag are in boldface type and italicized; the first three codons of the Kid-1 portion are underlined; numbering of amino acids is according to the rat Kid-1 protein as published in Ref. 15): pMT3/Kid-1, ATG **TAC CCA TAC GAT GTT CCA GAT TAC GCT** GGA ATT CCT CTA GAG GTC GAG GCC ACC **ATG GCT CCT** . . . (1–576); pMT3/Kid-1, A(–), ATG **TAC CCA TAC GAT GTT CCA GAT TAC GCT** GGA AAG CTT GGT ACC GAG CTC GGA TCC ACT AGT AAC GGC CGC CAG TGT GCT GGA ATT CTG CAG ATG GGA ATT TCC GGT GGT GGT GGA ATT CTA GAC **TCC ATG GCA** . . . (52–576); pMT3/Kid-1, AB(–), ATG **TAC CCA TAC GAT GTT CCA GAT TAC GCT** GGA ATT GAT CCC TGG . . . (72–576); pMT3/Kid-1C, ATG **TAC CCA TAC GAT GTT CCA GAT TAC GCT** GGA AAG CTT GGT ACC GAG CTC GGA TCC CCG GGA ATT TCC GGT GGT GGT GGT GGA **TCT TAT TTA** . . . (174–576); pMT3/Kid-1 (Zf 1–4), ATG **TAC CCA TAC GAT GTT CCA GAT TAC GCT** GGA AAG CTT GGT ACC GAG CTC GGA TCC CCG GGA ATT TCC GGT GGT GGT GGT GGA ATT CAT **AAA CGC TAT** . . . (186–299); pMT3/Kid-1 (Zf 5–13), ATG **TAC CCA TAC GAT GTT CCA GAT TAC GCT** GGA AAG CTT GGT ACC GAG CTC GGA TCC CCG GGA ATT TCC GGT GGT GGT GGT GGC **CGA GAA AAC** . . . (296–576).

Two additional plasmids were used: 1) pBXG1/Kid-1N, coding for a fusion protein between the DNA-binding domain of the yeast GAL4 protein and the NH<sub>2</sub> terminus of the rat Kid-1 protein without the zinc fingers (amino acids 1–195) (15); 2) pMT3A/KRIP-1, coding for KRIP-1 with an HA epitope tag at the NH<sub>2</sub> terminus (14).

**Preparation of Polyclonal Anti-Kid-1 and Anti-KRIP-1 Antibodies**—Fragments of the rat Kid-1 protein (amino acids 72–173) and the murine KRIP-1 protein (amino-terminal to the plant homeodomain (PHD) finger) were used to immunize rabbits according to standard protocols (16). The specificity of the antibodies was demonstrated on Western blots and by immunocytochemistry of transiently transfected COS-7 cells.

**Transient Expression Protocols**—COS-7 cells were transfected with 10–40 μg of expression plasmid according to the DEAE-dextran protocol (16). CV-1 cells were transfected with 20 μg of expression plasmid according to the DEAE-dextran (16) and the calcium phosphate protocols (17). LLC-PK<sub>1</sub> cells were transfected with 20 μg of expression plasmid according to the calcium phosphate protocol (17).

**Preparation of Nuclear Extracts**—Nuclear extracts were prepared as described by Hoppe-Seyler *et al.* (18). 2–3 days after transfection, COS-7 cells were washed twice with PBS and scraped into a microcentrifuge tube. The cells were centrifuged 5 min at 1250 × *g*, and the pellet was resuspended in lysis buffer (150 mM NaCl, 10 mM Tris, pH 7.9, 1 mM EDTA, pH 8.0, 0.6% Nonidet P-40). After an incubation of 5 min on ice, the cells were centrifuged 5 min at 1250 × *g*. The supernatant (containing cytoplasmic and detergent-soluble proteins) was saved, and the nuclear pellet was resuspended in nuclear extract buffer (1.5 mM MgCl<sub>2</sub>, 10 mM Hepes, pH 7.9, 0.1 mM EGTA, 0.1 mM EDTA, 0.5 mM dithiothreitol, 0.5 mM phenylmethylsulfonyl fluoride, 25% glycerol, 420 mM NaCl. Where indicated, 420 mM NaCl was substituted by 2 M NaCl and 2 M KCl, respectively). The nuclear suspension was incubated 20 min on ice and then centrifuged for 5 min at 14,000 × *g*. The supernatant (corresponding to the soluble nuclear fraction) was saved, and the remaining pellet was solubilized by sonication in PBS, 6 M urea.

To control for the role of the conformation of the zinc fingers, the nuclear extract buffer was modified by the addition of 0.1 mM *o*-phenanthroline; 0.1 mM *o*-phenanthroline, 50 mM EDTA; 50 mM EDTA; or 1 mg/ml *N*-ethylmaleimide, respectively. Otherwise, the protocol was followed as above.

For a DNase or RNase digest, the nuclei were resuspended in a buffer containing 10 mM Tris pH 7.0, 50 mM NaCl, 0.5% Triton X-100, 1 mM phenylmethylsulfonyl fluoride, 2 μg/ml aprotinin, 2 μg/ml leupeptin, 1 μg/ml pepstatin A. Then either DNase was added to 1 unit/ml or RNase A was added to 100 μg/ml, and RNase T was added to 40 units/μl (final concentration). The nuclear suspension was incubated 60 min at 37 °C before adding NaCl to a final concentration of 420 mM. After a 20-min incubation on ice, the nuclei were pelleted for 5 min at 4 °C, 14,000 × *g*. The supernatant (corresponding to the nuclear fraction) was saved, the remaining pellet was solubilized by sonication in PBS, 6 M urea.

Protein concentration in the different fractions was determined according to the method described by Bradford (19).

**Western Blot Analysis**—SDS-polyacrylamide gels and protein transfers were performed according to standard protocols with polyvinylidene difluoride membranes from Millipore (Eschborn, Germany) (16). After the transfer, membranes were blocked overnight at room temperature in PBS, 5% low fat dry milk, 0.5% Tween 20. The next morning, the membrane was incubated for 2 h at room temperature with the primary antibody, followed by a 1-h incubation with the secondary antibody. Immune complexes were detected with the Renaissance kit from NEN (Bad Homburg, Germany). The following primary antibodies were used: cell culture supernatant from the mouse anti-HA tag hybridoma 12CA5 diluted 1:25, cell culture supernatant from the mouse anti-Kid-1 hybridoma 5D12 (undiluted), a mouse monoclonal anti-lamin B antibody diluted 1:30 (kind gift of E. Brigitte Lane, University of Dundee, Dundee), and a human anti-NuMA antibody (20) diluted 1:1000 (kind gift of Herwig Ponstingl, German Cancer Research Center, Heidelberg). Horseradish peroxidase-conjugated secondary antibodies were goat anti-mouse IgG Fab used at a dilution of 1:10,000 and goat anti-human IgG Fab used at a dilution of 1:100,000 (Sigma, Deisenhofen, Germany).

**Single Antibody Immunocytochemistry of Transfected Cells**—One to two days after transfection, the cells were plated on coverslips and allowed to grow for an additional 1 or 2 days. Cells on coverslips were washed with PBS and then fixed 20 min in PBS containing 2% paraformaldehyde at room temperature. After a blocking step of 15 min in PBS containing 2% bovine serum albumin, 0.1% Triton X-100, the cells were incubated 2 h at room temperature with cell culture supernatant from the hybridoma 12CA5 (diluted 1:30 to 1:100; the 12CA5 antibody recognizes the HA tag). The primary antibody was washed off with PBS, after which the cells were incubated for 1 h at room temperature with the secondary antibody (fluorescein isothiocyanate-coupled goat anti-mouse IgG from Cappel (Eppelheim, Germany) diluted 1:100 or Cy3-coupled rat anti-mouse IgG from Dianova (Hamburg, Germany) diluted 1:300). After incubation with the secondary antibody, cells were stained for 2 min with the DNA-binding dye Hoechst 33258 (Sigma), washed three times for 5 min each with PBS, and mounted.

**Double Antibody Immunocytochemistry of Transfected Cells**—Cells were prepared as described for single antibody immunocytochemistry. For double-labeling experiments, cells were simultaneously incubated for 2 h at room temperature with the two primary antibodies. After three washes with 1× PBS, the primary antibodies were detected with fluorescein isothiocyanate-coupled goat anti-mouse IgG from Cappel (diluted 1:150), Cy3-coupled goat anti-human IgG from Dianova (diluted 1:300), and Cy3-coupled goat anti-rabbit IgG from Dianova, respectively. The following combinations of primary antibodies were used: cell culture supernatant of the mouse anti-HA tag hybridoma 12CA5 diluted 1:30 and a human anti-upstream binding factor (UBF) autoantibody diluted 1:300 (kind gift of Ingrid Grummt, German Cancer Research Center, Heidelberg); (NH<sub>4</sub>)<sub>2</sub>SO<sub>4</sub>-precipitated cell culture supernatant of the mouse anti-Kid-1 hybridoma 5D12 diluted 1:30; and rabbit anti-KRIP-1 antiserum diluted 1:30.

**Nucleolar Run-on**—Ongoing synthesis of rRNA in the nucleolus was visualized by incubating transfected COS-7 cells with bromo-UTP (21, 22). 48 h after the Me<sub>2</sub>SO shock, cells were rinsed twice each with 1× PBS and run-on buffer (20 mM Tris HCl, pH 7.4, 5 mM MgCl<sub>2</sub>, 0.5 mM EGTA, pH 8.0, 0.5 mM phenylmethylsulfonyl fluoride). The cells were permeabilized by incubating for 5 min with 0.05% Triton X-100 in run-on buffer. Following three washes with run-on buffer, the cells were incubated for 30 min at room temperature with 0.5 mM each of ATP, CTP, and GTP, 0.2 mM bromo-UTP, 50 mM (NH<sub>4</sub>)<sub>2</sub>SO<sub>4</sub>, 50 mM Tris-HCl, pH 7.4, 5 mM MgCl<sub>2</sub>, 0.1 mM EGTA, pH 8.0, and 10 μg/ml of amanitin (ATP, CTP, and GTP were purchased from Boehringer Mannheim, Mannheim, Germany; bromo-UTP and amanitin were purchased from Sigma). After the run-on reaction, the cells were rinsed again with 1× PBS, fixed for 20 min at room temperature with 2% paraformaldehyde, air-dried for 5 min, and then rinsed again twice with 1× PBS before staining with the primary antibodies. Newly synthesized rRNA and Kid-1 were detected as described under double antibody immunocytochemistry using a rabbit anti-Kid-1 antibody at a dilution of 1:1000 and a mouse monoclonal anti-bromodeoxyuridine antibody at a dilution of 1:50 (Dunn Labortechnik, Thelenberg, Asbach). Primary antibodies were detected with fluorescein isothiocyanate-coupled goat anti-mouse IgG from Cappel (diluted 1:150) and Cy3-coupled goat anti-rabbit IgG from Dianova (diluted 1:150).

<sup>1</sup> The abbreviations used are: HA, hemagglutinin; PBS, phosphate-buffered saline; UBF, upstream binding factor.

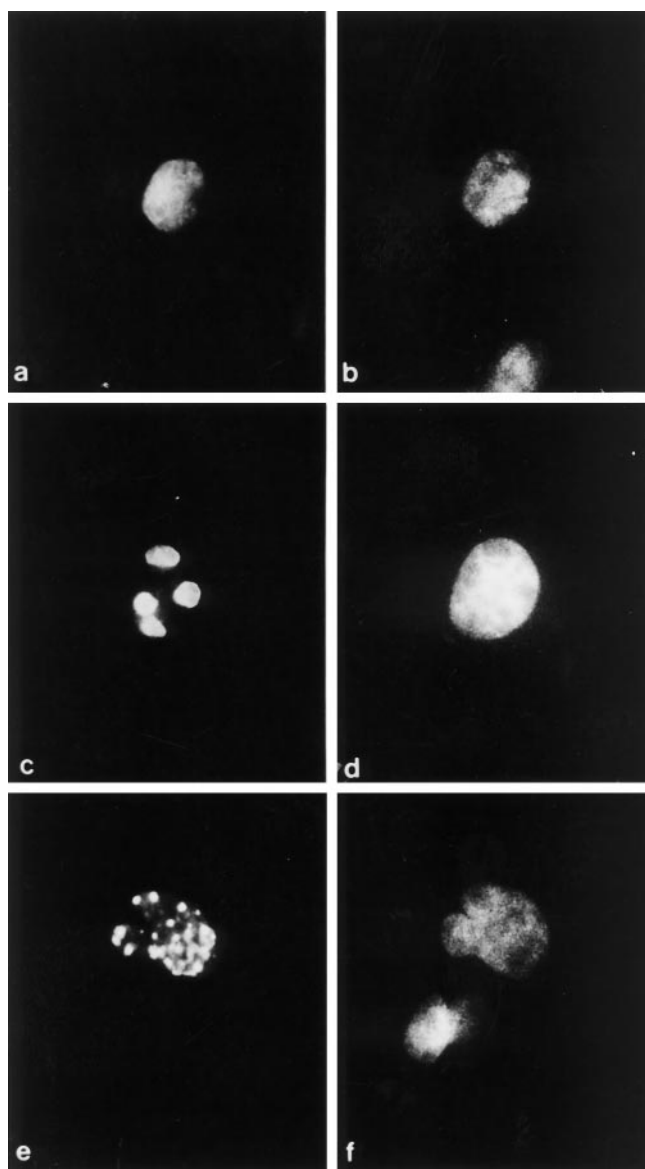


**FIG. 1. The rat Kid-1 protein is distributed in different nuclear domains.** COS-7 cells were transiently transfected with a plasmid encoding a full-length Kid-1 protein. The Kid-1 protein was tagged with an HA epitope of the influenza virus and could therefore easily be detected by immunofluorescence with the anti-HA epitope antibody 12CA5 (*a*, *c*, and *e*), while the nuclei were visualized with the dye Hoechst 33258 (*b*, *d*, and *f*). Immunofluorescence staining showed a homogeneous (*a*), patchy (*c*), and speckled (*e*) nuclear distribution of the Kid-1 protein. Magnification,  $\times 510$ .

## RESULTS

**Distribution of the Full-length Kid-1 and KRIP-1 Proteins in the Nucleus**—In order to determine the subcellular site of Kid-1 expression, COS-7 cells were transiently transfected with a plasmid encoding a full-length Kid-1 protein with an HA epitope tag at the NH<sub>2</sub> terminus. 2–3 days after the transfection, cells were stained with the anti-HA epitope antibody 12CA5 and a fluorescein isothiocyanate- or Cy3-coupled secondary antibody. By simultaneous staining of the transiently transfected cells with the DNA-binding dye Hoechst 33258, it could be clearly seen that Kid-1 was located in the nucleus. The distribution of Kid-1 inside the nucleus, however, varied between different transfected cells. Whereas some cells showed a homogeneous nuclear staining (Fig. 1, *a* and *b*), others presented with a patchy (Fig. 1, *c* and *d*) or speckled (Fig. 1, *e* and *f*) nuclear staining. In order to find out how the distribution of

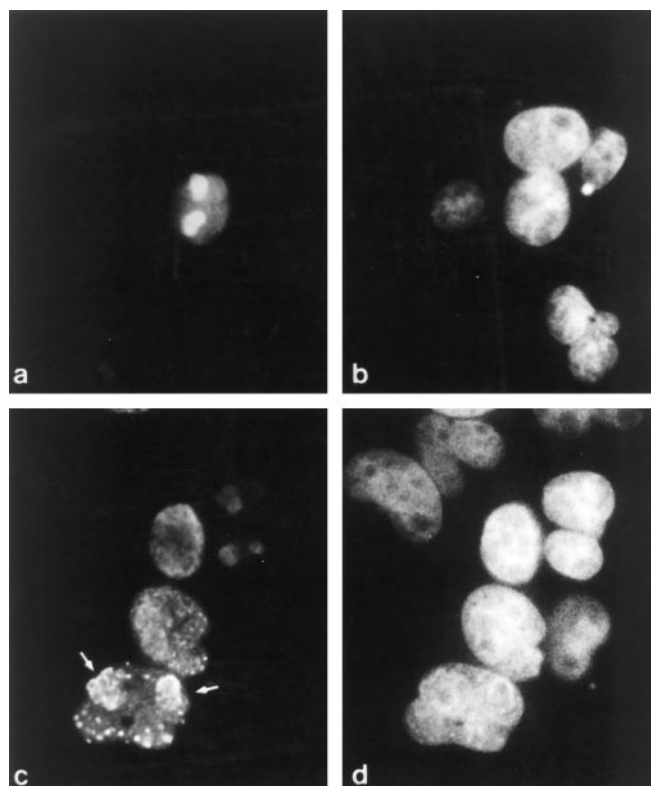


**FIG. 2. Time course of Kid-1 expression in COS-7 cells.** COS-7 cells were transfected with a Kid-1 expression plasmid and immunohistochemically stained 24 h (*a*) and 48 h (*c*) after the Me<sub>2</sub>SO shock, while nuclei were detected with the dye Hoechst 33258 (*b* and *d*). 24 h after the Me<sub>2</sub>SO shock, Kid-1 was expressed in patches (*a*), but at 48 h Kid-1 staining also appeared in nuclear speckles (*c*). Those speckles seemed to emanate from disintegrating patches (arrows in *c*). Magnification,  $\times 520$ .

Kid-1 changed depending on when the cells were harvested after the transfection, we stained transiently transfected COS-7 cells at various time points after the Me<sub>2</sub>SO shock treatment. Soon after the transfection (24 h after shock treatment), we only detected cells with a homogeneous and patchy distribution of Kid-1, and it was only at later time points that the speckles appeared (Fig. 2 and Table I). In some nuclei, it appeared as if the patches containing Kid-1 were disintegrating, so that speckles containing Kid-1 were generated (Fig. 2*c*). To learn more about the physiological relevance of the different expression patterns, COS-7 cells were transfected with a plasmid coding for an HA epitope-tagged KRIP-1 protein. KRIP-1 (also known as KAP-1 or TIF1 $\beta$ ) has been shown to interact with the KRAB-A domain of Cys<sub>2</sub>His<sub>2</sub>-zinc finger proteins and to mediate the transcriptional repressor activity of those proteins (12–14). KRIP-1 was also expressed in the nucleus, but was always distributed homogeneously in the nucleoplasm, obviously sparing the nucleoli (Fig. 3).

**The Kid-1 Protein Is Tightly Bound to Nuclear Structures, but KRIP-1 Is Not**—COS-7 cells, which were transfected with the expression plasmid coding for a HA-Kid-1 fusion protein, were subjected to a standard nuclear extraction protocol with 420 mM NaCl. The Kid-1 protein was not present in the cytosolic nor the nuclear extracts but was found in the insoluble pellet fraction remaining after the nuclear extraction. When the pellet was solubilized with 6 M urea and the proteins contained in the pellet fraction were separated on a denaturing polyacrylamide gel, a single band could be observed with the anti-HA-epitope antibody, whereas extracts from mock-transfected COS-7 cells were unreactive with the anti-HA epitope antibody (Fig. 4*a*). The observed relative molecular weight of

TABLE I  
COS-7 cells transfected with pMT3/Kid-1

24, 39, and 48 h after the Me<sub>2</sub>SO shock, cells were stained with the monoclonal anti-HA epitope antibody 12CA5. 100 positive nuclei were evaluated according to the nuclear distribution of the Kid-1 protein.

Time	Hom <sup>a</sup>	Hom/patches <sup>b</sup>	Patches/speckles <sup>c</sup>	Speckles <sup>d</sup>
24 h	4	96		
39 h	10	72	15	3
48 h	3	57	36	4

<sup>a</sup> Strictly homogeneous distribution.

<sup>b</sup> Hom/patches, patches in combination with homogeneous distribution.

<sup>c</sup> Patches/speckles, patches combined with speckles.

<sup>d</sup> Speckles, only speckled distribution.

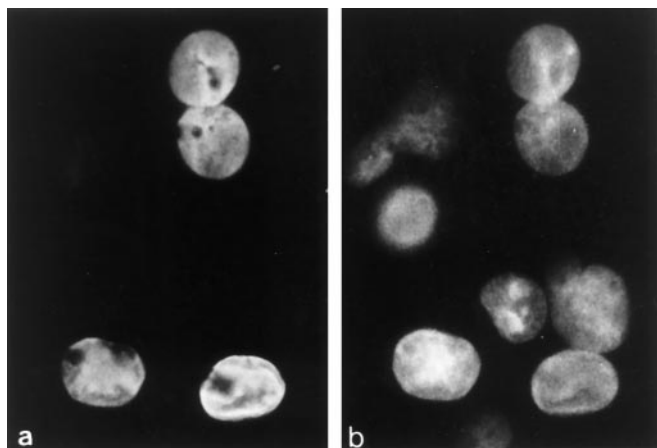


FIG. 3. **KRIP-1 is a nuclear protein with a homogeneous distribution.** KRIP-1 was transiently expressed in COS-7 cells. Due to an HA-epitope tag at the NH<sub>2</sub> terminus, the KRIP-1 protein could be visualized by immunofluorescence staining with the antibody 12CA5 (a), and nuclei were stained with Hoechst 33258 (b). The KRIP-1 protein was always homogeneously distributed in nuclei of transfected cells, apparently sparing the nucleoli. Magnification,  $\times 520$ .

the HA-Kid-1 fusion protein of approximately 59 kDa was smaller than the calculated relative molecular weight of 68.4 kDa. In order to control our nuclear extraction protocol for its efficiency, we also transiently expressed the HA-tagged KRIP-1 protein in COS-7 cells. The KRIP-1 protein was easily detected in the nuclear extract and appeared to a large extent already in the detergent-soluble fraction (Fig. 4b).

It has been reported that the treatment of nuclei with high concentrations of salt (2 M NaCl) results in the release of most nuclear proteins but leaves behind proteins constituting the nuclear matrix or proteins tightly associated with it (23). Treatment of transfected COS-7 cells with 2 M NaCl and 2 M KCl, however, did not release the Kid-1 protein from the nuclei, suggesting that Kid-1 adheres strongly to the nuclear matrix (Fig. 5b). Incubation of the nuclei with the SH group modifying agent *N*-ethylmaleimide, the divalent cation chelator EDTA and the Zn<sup>2+</sup> chelator *o*-phenanthroline also did not result in the release of the Kid-1 protein from the nuclei (Fig. 5a), nor did a digest of the nuclei with DNase and RNase change the distribution pattern of Kid-1 (Fig. 5c). In order to control for the integrity of the protein preparations, the blots were also probed with antibodies against lamin and NuMA, two nuclear matrix-associated proteins (24–26). With either antibody, a distinct band was detected predominantly in the insoluble fraction after RNase treatment, thus validating our extracts (Fig. 5d).

*The Larger Zinc Finger Cluster of Kid-1 Serves as a Nuclear Targeting Signal, whereas the KRAB-A Domain Is Responsible for the Disintegration of the Nucleolus*—The Kid-1 protein contains highly conserved KRAB-A and -B domains at its NH<sub>2</sub> terminus and 13 Cys<sub>2</sub>His<sub>2</sub>-zinc fingers clustered in groups of

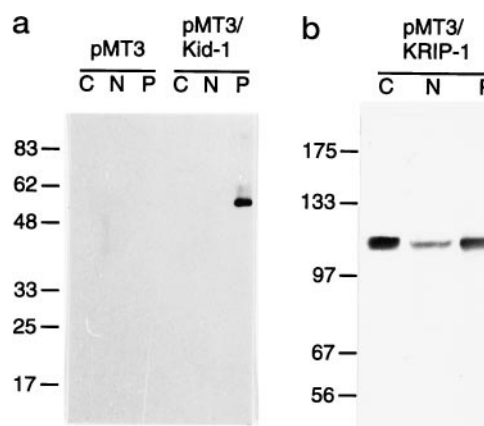
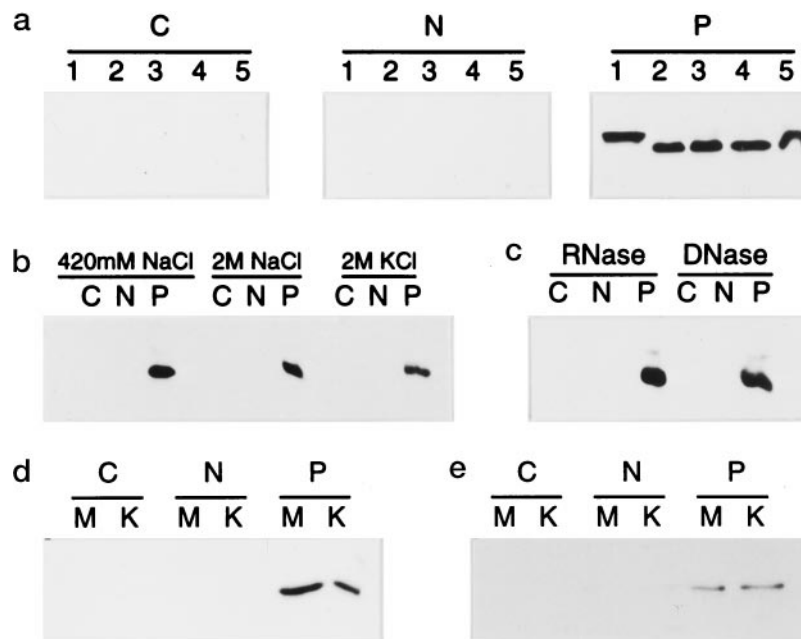


FIG. 4. **The Kid-1 protein is tightly associated with nuclear structures, but KRIP-1 is not.** Transiently transfected COS-7 cells were lysed with Nonidet P-40, and the nuclei were separated from the detergent-soluble proteins by centrifugation. The nuclei were extracted with a buffer containing 420 mM NaCl, which yielded a fraction with soluble and “insoluble” nuclear proteins. Insoluble proteins were homogenized by sonication in PBS, 6 M urea. Proteins were separated on a SDS-polyacrylamide gel, transferred to a polyvinylidene difluoride membrane, and stained with the anti-HA epitope antibody 12CA5. Whereas Kid-1 was found in the fraction comprising the insoluble nuclear proteins (a), a large portion of the KRIP-1 protein could already be detected in the fraction containing the detergent-soluble proteins (b). COS-7 cells transfected with the wild-type expression vector pMT3 showed no staining. C, detergent-soluble proteins; N, soluble nuclear proteins; P, insoluble nuclear proteins.

four and nine zinc fingers at its COOH terminus. Whereas the KRAB-A domain has been identified as a protein-protein interaction motif (12–14), the zinc fingers of Kid-1 have been shown to recognize heteroduplex DNA (27). As a first approach to determine the functional significance of the various motifs in the Kid-1 protein, we substituted the zinc finger domain of Kid-1 with the zinc fingers of the yeast transcription factor GAL4. The DNA-binding domain of GAL4 contains zinc fingers of the C<sub>6</sub> class; furthermore, there are no known binding sites for GAL4 in the mammalian genome (28). Transient transfections of COS-7 cells with the plasmid pBXG1/Kid-1N, which codes for a fusion protein between the DNA-binding domain of yeast GAL4 and the non-zinc finger portion of rat Kid-1, resulted in a different staining pattern when compared with COS-7 cells transfected with pMT3/Kid-1. Transfection of cells with pBXG1/Kid-1N yielded a homogeneous nuclear staining; a speckled or patchy pattern like that observed in cells transfected with pMT3/Kid-1 was never detected (data not shown). Treatment of nuclei with a buffer containing 420 mM NaCl resulted in the extraction of a sizable portion of the GAL4/Kid-1 fusion protein into the soluble fraction (data not shown).

The results obtained with the GAL4/Kid-1 fusion protein suggested that the zinc fingers of Kid-1 are important for the nonhomogeneous distribution of the full-length Kid-1 protein in the nucleus and its tight association to nuclear structures. In order to provide direct evidence for that assumption, we generated mutant Kid-1 proteins with consecutively larger deletions from the NH<sub>2</sub> terminus. Because these mutant proteins were tagged with the HA epitope, they could easily be detected by immunofluorescence and on a Western blot. A Kid-1 mutant protein lacking the KRAB-A domain was sorted to the nucleus (Fig. 6, a and b), but it was distributed in patches, and we never noticed those larger speckles seen with the full-length Kid-1 protein (approximately 1/4 the diameter of an intact nucleolus; see below) but only much smaller ones (approximately 1/20 the diameter of an intact nucleolus; not shown) in about 40–45% of the transfected cells. Further deletion of the KRAB-B domain did not change the overall distribution of the mutant Kid-1



**FIG. 5. Evidence for the binding of Kid-1 to the nuclear matrix.** COS-7 cells were transiently transfected with pMT3/Kid-1 (encoding an HA epitope-tagged full-length Kid-1 protein). Transfected cells were subjected to various nuclear extraction protocols described below, and the fractions were analyzed by Western blot with the anti-Kid-1 antibody 5D12. *a*, when the nuclei of COS-7 cells expressing a full-length Kid-1 protein were treated with 1 mg/ml *N*-ethylmaleimide (*lane 1*); a combination of 0.1 mM *o*-phenanthroline, 50 mM EDTA (*lane 2*); 50 mM EDTA (*lane 3*); and 0.1 mM *o*-phenanthroline (*lane 4*), Kid-1 still remained in the pellet fraction. *Lane 5* represents fractions obtained with the regular nuclear extraction protocol using 420 mM NaCl but without the addition of any of the aforementioned chemicals. The protein in *lane 1* exhibits a higher molecular weight due to the alkylation of the cysteine residues of Kid-1 by *N*-ethylmaleimide. *b*, neither extraction with a buffer containing 2 M NaCl nor a buffer containing 2 M KCl resulted in the release of the full-length Kid-1 protein from the nuclei; the different fractions obtained with a buffer containing 420 mM NaCl are shown for comparison. *c*, when nuclei of COS-7 cells transfected with pMT3/Kid-1 were digested with 1 unit/ml DNase or a combination of RNase A (100  $\mu$ g/ml) and RNase T (40 units/ $\mu$ l), the full-length Kid-1 protein still remained in the insoluble pellet fraction. *d* and *e*, in order to control for the integrity of the extract preparation in the presence of RNase, the blots were also probed with antibodies against lamin B (*d*) and NuMA (*e*), two nuclear matrix-associated proteins. Even after a digest with RNase, both proteins remained predominantly in the insoluble fraction no matter whether mock-transfected (*M*) or Kid-1-expressing COS-7 cells (*K*) were used, although after a longer exposure they could also be detected in the other fractions. *C*, detergent-soluble proteins; *N*, soluble nuclear proteins; *P*, insoluble nuclear proteins; *M*, mock-transfected COS-7 cells; *K*, COS-7 cells transfected with the Kid-1 expression plasmid pMT3/Kid-1.

protein (Fig. 6, *d* and *e*). This expression pattern was maintained when mutant Kid-1 proteins containing all 13 zinc fingers (Fig. 6, *g* and *h*) or only the second zinc finger cluster containing zinc fingers 5–13 were expressed in COS-7 cells (Fig. 6, *m* and *n*). The first zinc finger cluster comprising zinc fingers 1–4 was sorted to the nucleus but was always distributed homogeneously in the nucleus (Fig. 6, *j* and *k*).

The expression patterns of the various Kid-1 mutants correlated well with their extractability from the nucleus. All of the mutants containing zinc fingers 5–13 could only inefficiently be extracted from the nucleus, whereas the mutant protein comprising the first four zinc fingers could easily be extracted. The presence of the KRAB-A and KRAB-B domains had no influence on the extractability of the proteins from the nucleus (Fig. 6, *c*, *f*, *i*, *l*, and *o*).

In order to identify the nuclear compartment(s) Kid-1 was targeted to, we used antibodies against various nuclear structures in double-labeling experiments. Staining with a human autoantibody against the nucleolar transcription factor UBF resulted in a perfect colocalization with the Kid-1 protein in patches, identifying the patches as nucleoli (Fig. 7, *a* and *b*). In nuclei with a speckled distribution of Kid-1, UBF was also located in speckles, although the intensity of UBF staining clearly was less than in intact nucleoli, and some speckles even lacked UBF staining altogether (Fig. 7, *c* and *d*). The mutant comprising zinc fingers 5–13 colocalized perfectly with UBF, thus identifying the larger zinc finger cluster of Kid-1 as a nucleolar targeting domain (Fig. 7, *e* and *f*). The results obtained in COS-7 cells were corroborated by transiently expressing the Kid-1 mutant comprising zinc fingers 5–13 in CV-1 cells

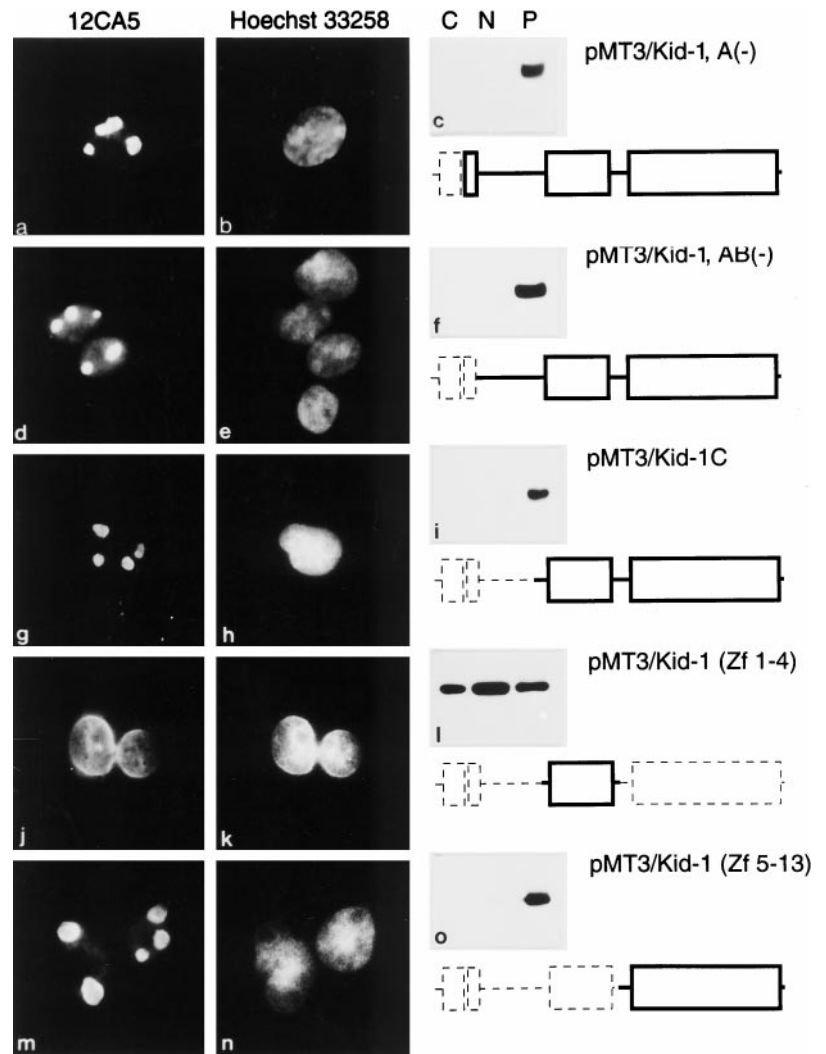
and LLC-PK<sub>1</sub> cells. The CV-1 cell line represents the parent cell line of COS-7 cells (29); it does not express the large T antigen of SV40, and therefore the expression levels of exogenous proteins, encoded by plasmids with an SV40 origin of replication, are much lower than in COS-7 cells. Both in CV-1 cells and LLC-PK<sub>1</sub> cells, a highly differentiated porcine renal epithelial cell line (30), the larger zinc finger cluster of Kid-1 was sorted to the nucleolus, indicating that the nucleolar expression pattern of Kid-1 did not depend on its expression level (Fig. 8).

**Transcription of the rDNA Genes Is Shut Off in Nucleolar Fragments**—Expression of the Kid-1 mutant lacking only the KRAB-A domain did not result in nucleolar disintegration, arguing that transcriptional repression was necessary for this phenomenon. It was puzzling, however, that KRIP-1, the adaptor protein for KRAB-zinc finger proteins, was located in the nucleoplasm and not in the nucleoli in the absence of Kid-1 (Fig. 3). We therefore cotransfected Kid-1 and KRIP-1 to determine whether Kid-1 could influence the location of KRIP-1. Interestingly, in cells coexpressing Kid-1 and KRIP-1, KRIP-1 was indeed sorted to the nucleoli (Fig. 9, *a* and *b*). The hypothesis, that Kid-1 repressed rDNA transcription through its adaptor protein KRIP-1, was directly tested by performing nucleolar run-ons with bromo-UTP either in the absence or presence of Kid-1. Ongoing synthesis of rRNA was detected in intact nucleoli (“patches”), whereas in nucleolar fragments (“speckles”) rRNA synthesis was greatly diminished (Fig. 9, *c–f*).

#### DISCUSSION

When the HA epitope-tagged full-length rat Kid-1 protein was transiently expressed in COS-7 cells, immunocytochemical

**FIG. 6. The nine-zinc finger cluster of Kid-1 is responsible for the patchy distribution and tight association in the nucleus.** HA epitope-tagged Kid-1 mutant proteins were transiently transfected into COS-7 cells and detected by immunofluorescence (*a, d, g, j, and m*), while nuclei were stained with Hoechst 33258 (*b, e, h, k, and n*). Mutant proteins containing the nine-zinc finger cluster are distributed in patches (*a, d, g, and m*), whereas the four-zinc finger cluster is distributed homogeneously (*j*) in nuclei. The patchy distribution correlates well with the tight association to as yet unidentified nuclear structures. This is demonstrated by Western blot analysis of nuclear extracts from COS-7 cells transiently transfected with the same constructs (*c, f, i, l, and o*). The KRAB-A domain, KRAB-B domain, and four- and nine-zinc finger clusters (from NH<sub>2</sub> to COOH terminus) are shown as *boxes*, and deleted portions of the Kid-1 protein are indicated by *dashed lines*. C, detergent-soluble proteins; N, soluble nuclear proteins; P, insoluble nuclear proteins. Magnification,  $\times 400$ .



analysis showed patchy and speckled expression patterns of Kid-1 in the nucleus. Using a human autoantibody against the nucleolar transcription factor UBF, a clear colocalization of Kid-1 and UBF in patches was detected, demonstrating that the full-length Kid-1 protein is sorted to the nucleolus. The nucleolus consists of at least three ultrastructurally defined compartments: a fibrillar center, a dense fibrillar component, and a granular component, which contain distinct proteins and serve specific functions (for reviews, see Refs. 31–33). Transcription of the rDNA genes in the nucleolus depends on the presence of UBF, the TATA-binding protein, and three TATA-binding protein-associated factors. UBF belongs to the HMG box family of transcription factors and has been cloned from a variety of different species (*e.g.* Refs. 34 and 35). The DNA binding characteristics of UBF are remarkable, because so far no sequence-specific binding to DNA could be demonstrated; UBF rather exhibits an affinity for cruciform DNA (36–38). We have recently shown that both zinc finger clusters of Kid-1 also can bind in an apparently sequence-independent manner to heteroduplex or “bubble” DNA (27), but clearly this property is not sufficient to confer sorting of Kid-1 to the nucleolus, because only the larger zinc finger cluster comprising zinc fingers 5–13 is required for nucleolar targeting, whereas the smaller zinc finger cluster of Kid-1 was distributed homogeneously in the nucleus. The importance of the zinc finger domains of Kid-1 becomes even more evident by the fact that the rat, murine, and human homologues of Kid-1 possess a very high homology in their zinc finger regions and also share the same arrange-

ment of the zinc fingers in clusters of four and nine zinc fingers (15, 39, 40). Therefore, although both zinc finger clusters obviously contain nuclear localization signals similar to what has been described for other zinc finger proteins (*e.g.* Refs. 41 and 42) and both of them can bind to heteroduplex DNA (27), they are functionally different. A similar picture has emerged for UBF insofar as only the first HMG box is required (together with the acidic tail of UBF) for nucleolar sorting (43), but the other HMG boxes of UBF can bind to DNA as well (44, 45). So far we do not know the nature of this additional signal with respect to Kid-1, but clearly it has to reside in the large zinc finger cluster. Interestingly, the large zinc finger cluster of Kid-1 also was responsible for the tight association inside the nucleus to as yet unknown structures. In the case of UBF, a tight nuclear association has been described for UBF in mitotic cells as compared with cells in interphase; on a biochemical level, it is the phosphorylated form of UBF that can be hardly extracted from the nucleus (46). For both Kid-1 and UBF, it is unknown how this tight association is mediated.

While the patchy distribution of the Kid-1 protein could be detected early after the Me<sub>2</sub>SO shock, the appearance of the speckles was a late event after transfection, with the speckles emanating from disintegrating patches. The double staining with the anti-UBF antibody showed that the patchy distribution of Kid-1 corresponds to intact nucleoli, while the speckles represent disintegrated nucleoli. The disintegration of the nucleoli depends on the presence of the KRAB-A domain, because transfection of cells with a mutant lacking the KRAB-A domain

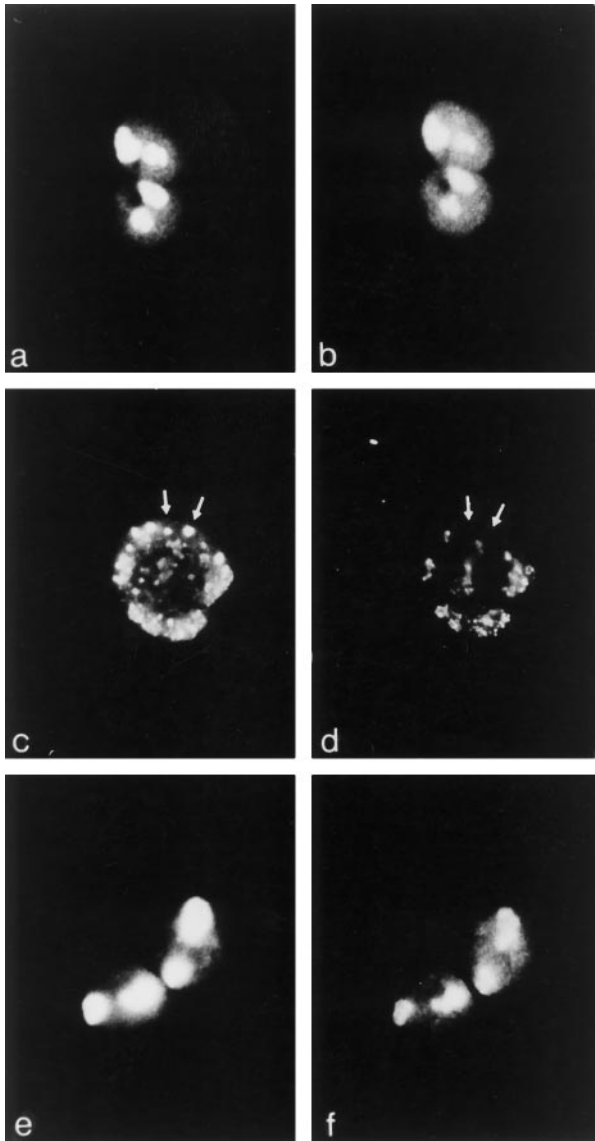


**FIG. 7. The nine-zinc finger cluster of Kid-1 can serve as a nucleolar targeting signal.** COS-7 cells were transiently transfected with a plasmid coding for an HA-tagged full-length Kid-1 protein (*a–d*) and with a plasmid coding for an HA-tagged Kid-1 mutant protein comprising zinc fingers 5–13 (*e* and *f*). Double staining with a human anti-UBF antibody (*b*, *d*, and *f*) and the mouse monoclonal anti-HA epitope antibody 12CA5 (*a*, *c*, and *e*) clearly demonstrated the colocalization of the Kid-1 proteins and UBF in intact nucleoli (*a* and *b*, *e* and *f*). In cells showing a speckled distribution of the full-length Kid-1 protein, some of the speckles still contained Kid-1 but had lost UBF (arrows in *c* and *d*). Magnification,  $\times 600$ .

resulted in a patchy staining pattern. The KRAB-A domain is a potent transcriptional repressor motif (3–6), and the disintegration of the nucleolus by Kid-1 therefore probably depends on the transcriptional repression characteristics of Kid-1. This also explains the time-dependent increase in the number of cells with nucleolar fragments, because it requires some time before Kid-1 is expressed, before it shuts off transcription in the nucleolus and before the nucleolus disintegrates. Such a model is in some contrast to the data presented by Moosmann *et al.* (10), who showed that the KRAB-A domain did not repress transcription mediated by RNA polymerase I. In their study, however, they used fusion proteins between the KRAB-A domain and the DNA-binding domains of LexA and GAL4 on the one hand and a reporter plasmid containing only a short fragment of the human rDNA gene promoter on the other hand

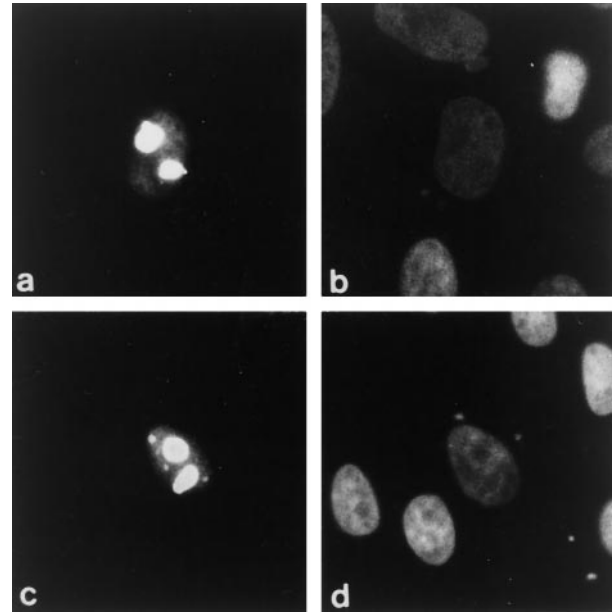


**FIG. 8. The nine-zinc finger cluster of Kid-1 can serve as a nucleolar targeting signal also in CV-1 cells and LLC-PK<sub>1</sub> cells.** CV-1 cells (*a*, *b*) and LLC-PK<sub>1</sub> cells (*c*, *d*) were transiently transfected with an expression plasmid coding for the HA epitope-tagged large zinc finger cluster of Kid-1. It can be easily seen that also in these cell lines the mutant comprising zinc fingers 5–13 was sorted to the nucleolus as demonstrated by immunocytochemical staining with the anti-HA-epitope antibody 12CA5 (*a* and *c*). Nuclei were counterstained with Hoechst 33258 (*b* and *d*). Magnification,  $\times 600$ .

(10). Because we looked at the effect of the wild-type Kid-1 protein on nucleolar integrity, our studies were conducted in a more natural context, where additional cofactors for the repression of nucleolar transcription may be present. Although there remains the possibility that the nucleolar disintegration caused by the KRAB-A domain is not based on transcriptional repression, we consider this unlikely in light of the well established transcriptional repressor effects by KRAB-A domains from a variety of different proteins (3–6) and by two additional pieces of evidence. Whereas in the absence of Kid-1 KRIP-1 was located in the nucleoplasm and not in the nucleolus, coexpression of Kid-1 resulted in the rerouting of KRIP-1 into the nucleolus. Most importantly, ongoing rRNA synthesis in nucleolar fragments (speckles) with Kid-1 labeling was greatly repressed, arguing that transcription of the rDNA genes was shut off. This was not an immediate effect, however, because rRNA synthesis could still be demonstrated in intact nucleoli (patches) with Kid-1 labeling.

Nucleolar fragments can also be observed under other circumstances (*e.g.* during apoptosis (47), at the end of mitosis, or experimentally induced). During the cell cycle, the nucleoli disassemble at prophase and reappear in telophase, when they are reassembled from the nucleolus organizer region and prenucleolar bodies. The nucleolus organizer region contains proteins of the rDNA transcriptional machinery such as RNA polymerase I and UBF (*e.g.* Refs. 48–50), which remain bound to the nucleolus organizer region even during mitosis. Prenucleolar bodies, however, appear *de novo* in late mitosis and contain primarily proteins of the dense fibrillar component such as fibrillarlin, nucleolin, and B23/NO38 (summarized in Ref. 51). The coalescence of nucleolus organizer regions and prenucleolar bodies can be prevented by the DNA topoisomerase I inhibitor camptothecin (52) and by microinjecting antibodies against RNA polymerase I into mitotic cells (53), which points to the importance of rDNA gene transcription in the reformation of the nucleolus. Incubation of cells with the aden-

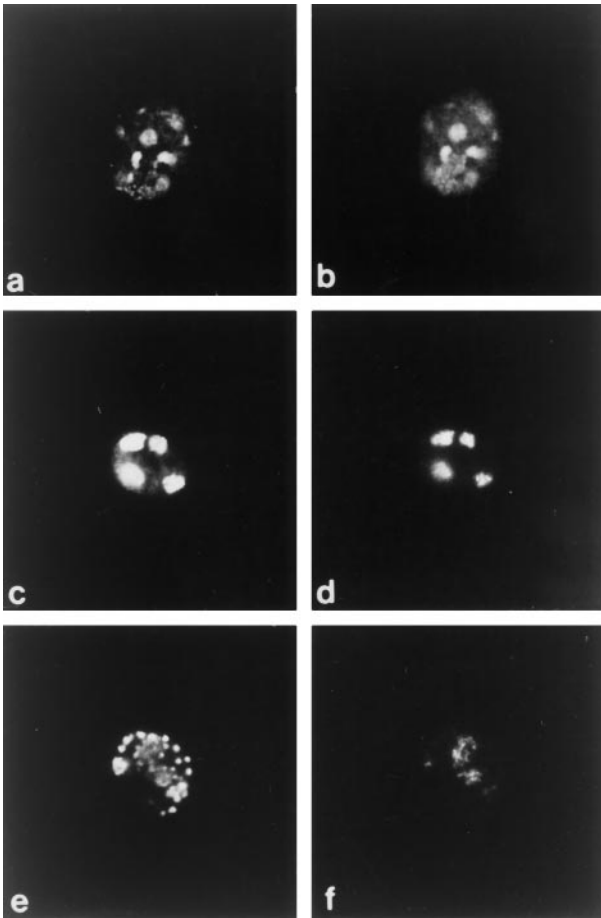


**FIG. 9. Transcription of rDNA is shut off by the expression of Kid-1.** *a* and *b*, in order to determine how the expression of Kid-1 affected the distribution of KRIP-1, both proteins were simultaneously expressed in COS-7 cells. Using double antibody immunocytochemistry, the Kid-1 protein was detected with the mouse monoclonal anti-Kid-1 antibody 5D12 (*a*) and KRIP-1 with a polyclonal rabbit anti-KRIP-1 antiserum (*b*). Upon expression of Kid-1, KRIP-1 could also clearly be detected in the nucleolus, although the nucleoplasmic staining was still present. *c-f*, the effect of the expression of Kid-1 in COS-7 cells on rDNA transcription was investigated by nucleolar run-ons. Ongoing rRNA synthesis in the nucleolus was demonstrated by incubating COS-7 cells with bromo-UTP in the presence of  $\alpha$ -amanitin to inhibit RNA-polymerase II and subsequent immunocytochemistry with a mouse monoclonal anti-bromodeoxyuridine antibody. Expression of Kid-1 was simultaneously detected with a polyclonal rabbit anti-Kid-1 antiserum. rRNA was still synthesized (*d*) in intact nucleoli containing Kid-1 (*c*), whereas in disintegrating nucleoli containing Kid-1 (*e*) the synthesis of rRNA was diminished in the remaining intact nucleoli and almost absent in the nucleolar fragments (*f*). Magnification,  $\times 600$ .

osine analogue 5,6-dichloro-1- $\beta$ -D-ribofuranosylbenzimidazole, which suppresses mRNA synthesis but does not inhibit or only moderately inhibits rRNA synthesis, leads to the disintegration of the nucleolus into a structure called the nucleolar necklace (54). In contrast to prenucleolar bodies, the nuclear necklace still contains RNA polymerase I (55). At this point, we do not know whether the speckles generated by the expression of Kid-1 correspond to any of those structures. The disappearance of UBF from some of the speckles containing Kid-1 would argue that those speckles correspond to prenucleolar bodies. Interestingly, one of the mechanisms by which UBF activates transcription of the rDNA genes probably lies in the replacement of the Ku antigen, a negative regulator of rDNA gene transcription, from the rDNA promoter (56). It therefore seems possible that Kid-1 can replace UBF from the rDNA promoter, but clearly more markers are needed to characterize the nature of the Kid-1 speckles.

At this point, we do not know in which biological context Kid-1 exerts its function. Previous studies have shown that Kid-1 is connected to heterochromatin through its adaptor protein KRIP-1 (12–14, 57). The connection between the nucleolus and heterochromatin has also been made for Modulo, a modifier of position-effect variegation in *Drosophila* (58), and for Zfp37, a murine Cys<sub>2</sub>His<sub>2</sub>-zinc finger protein with a truncated KRAB-A domain that is expressed in neuronal cells (59). In the case of Modulo, it has been hypothesized that the nucleolus balances the amount of Modulo available for heterochromatin formation and position-effect variegation (58). Besides Kid-1 and Zfp37, three other zinc finger proteins have been reported to reside in the nucleolus so far. LYAR, a protein with a potential RING finger motif (60), has been shown to enhance tumor formation (61), whereas PAG608, a protein with three Cys<sub>2</sub>His<sub>2</sub>-zinc fingers, can promote apoptosis (62). So far, no effect on growth has been reported for MOK2, another Cys<sub>2</sub>His<sub>2</sub>-zinc finger protein shown to reside in the nucleolus (63). Because of the shutdown of nucleolar transcription by Kid-1 and the vital role of rRNA synthesis for a cell, it is likely that Kid-1 also affects cell growth. Interestingly, disintegration of the nucleolus represents one of the earliest morphological changes during apoptotic cell death (47). In addition to Kid-1, a speckled distribution has also been reported for the KRAB-zinc finger proteins ZNF74 (25) and Zfp59 (64), but both ZNF74 and Zfp59 only contain a truncated KRAB-A domain at their NH<sub>2</sub> termini, which very likely is inactive so that the respective zinc finger domains probably are important for the targeting of either protein to its specific nuclear compartment. More information about the protein network, which these zinc finger proteins are part of, will help us to better understand their function in molecular and cell biological terms.

**Acknowledgments**—We acknowledge the kind gifts of materials from John Kyriakis (pMT3), Ingrid Grummt (anti-UBF antiserum), Herwig Ponstingl (anti-NuMA antiserum), and E. Brigitte Lane (anti-lamin B antibody) without which this work would not have been possible. We thank Rachel Gallagher for critically reading the manuscript. The expert photographic work of Ingrid Ertel and graphics of Rolf Nonnenmacher are gratefully acknowledged.

#### REFERENCES

- Hanna-Rose, W., and Hansen, U. (1996) *Trends Genet.* **12**, 229–234
- Kamakaka, R. T. (1997) *Trends Biochem. Sci.* **22**, 124–128
- Margolin, J. F., Friedman, J. R., Meyer, W. K.-H., Vissing, H., Thiesen, H.-J., and Rauscher, F. J., III. (1994) *Proc. Natl. Acad. Sci. U. S. A.* **91**, 4509–4513
- Witzgall, R., O'Leary, E., Leaf, A., Önal, D., and Bonventre, J. V. (1994) *Proc. Natl. Acad. Sci. U. S. A.* **91**, 4514–4518
- Pengue, G., Calabrò, V., Bartoli, P. C., Pagliuca, A., and Lania, L. (1994) *Nucleic Acids Res.* **22**, 2908–2914
- Vissing, H., Meyer, W. K.-H., Aagaard, L., Tommerup, N., and Thiesen, H.-J. (1995) *FEBS Lett.* **369**, 153–157
- Bellefroid, E. J., Poncet, D. A., Lecocq, P. J., Revelant, O., and Martial, J. A. (1991) *Proc. Natl. Acad. Sci. U. S. A.* **88**, 3608–3612
- Rosati, M., Marino, M., Franze, A., Tramontano, A., and Grimaldi, G. (1991) *Nucleic Acids Res.* **19**, 5661–5667
- Bellefroid, E. J., Lecocq, P. J., Benhida, A., Poncet, D. A., Belayew, A., and Martial, J. A. (1989) *DNA* **8**, 377–387
- Moosmann, P., Georgiev, O., Thiesen, H.-J., Hagmann, M., and Schaffner, W. (1997) *Biol. Chem.* **378**, 669–677
- Pengue, G., and Lania, L. (1996) *Proc. Natl. Acad. Sci. U. S. A.* **93**, 1015–1020
- Friedman, J. R., Fredericks, W. J., Jensen, D. E., Speicher, D. W., Huang, X.-P., Neilson, E. G., and Rauscher, F. J., III (1996) *Genes Dev.* **10**, 2067–2078
- Moosmann, P., Georgiev, O., Le Douarin, B., Bourquin, J.-P., and Schaffner, W. (1996) *Nucleic Acids Res.* **24**, 4859–4867
- Kim, S.-S., Chen, Y.-M., O'Leary, E., Witzgall, R., Vidal, M., and Bonventre, J. V. (1996) *Proc. Natl. Acad. Sci. U. S. A.* **93**, 15299–15304
- Witzgall, R., O'Leary, E., Gessner, R., Ouellette, A. J., and Bonventre, J. V. (1993) *Mol. Cell. Biol.* **13**, 1933–1942
- Ausubel, F. A., Brent, R., Kingston, R. E., Moore, D. D., Seidman, J. G., Smith, J. A., and Struhl, K. (eds) (1996) *Current Protocols in Molecular Biology*, John Wiley & Sons, Inc., New York
- Chen, C., and Okayama, H. (1987) *Mol. Cell. Biol.* **7**, 2745–2752
- Hoppe-Seyler, F., Butz, K., Rittmüller, C., and von Knebel Doeberitz, M. (1991) *Nucleic Acids Res.* **19**, 5080
- Bradford, M. M. (1976) *Anal. Biochem.* **72**, 248–254
- Kempf, T., Bischoff, F. R., Kalies, I., and Ponstingl, H. (1994) *FEBS Lett.* **354**,

- 307–310
21. Jackson, D. A., Hassan, A. B., Errington, R. J., and Cook, P. R. (1993) *EMBO J.* **12**, 1059–1065
  22. Masson, C., Bouniol, C., Fomproix, N., Szöllösi, M. S., Debey, P., and Hernandez-Verdun, D. (1996) *Exp. Cell Res.* **226**, 114–125
  23. He, D., Nickerson, J. A., and Penman, S. (1990) *J. Cell Biol.* **110**, 569–580
  24. Hozák, P., Sasseville, A. M.-J., Raymond, Y., and Cook, P. R. (1995) *J. Cell Sci.* **108**, 635–644
  25. Grondin, B., Bazinet, M., and Aubry, M. (1996) *J. Biol. Chem.* **271**, 15458–15467
  26. Cleveland, D. W. (1995) *Trends Cell Biol.* **5**, 60–64
  27. Elser, B., Kriz, W., Bonventre, J. V., Englert, C., and Witzgall, R. (1997) *J. Biol. Chem.* **272**, 27908–27912
  28. Johnson, P. F., and McKnight, S. L. (1989) *Annu. Rev. Biochem.* **58**, 799–839
  29. Gluzman, Y. (1981) *Cell* **23**, 175–182
  30. Hull, R. N., Cherry, W. R., and Weaver, G. W. (1976) *In Vitro* **12**, 670–677
  31. Goessens, G. (1984) *Int. Rev. Cytol.* **87**, 107–158
  32. Scheer, U., Thiry, M., and Goessens, G. (1993) *Trends Cell Biol.* **3**, 236–241
  33. Shaw, P. J., and Jordan, E. G. (1995) *Annu. Rev. Cell Dev. Biol.* **11**, 93–121
  34. Jantzen, H.-M., Admon, A., Bell, S. P., and Tjian, R. (1990) *Nature* **344**, 830–836
  35. Hisatake, K., Nishimura, T., Maeda, Y., Hanada, K., Song, C.-Z., and Muramatsu, M. (1991) *Nucleic Acids Res.* **19**, 4631–4637
  36. Copenhaver, G. P., Putnam, C. D., Denton, M. L., and Pikaard, C. S. (1994) *Nucleic Acids Res.* **22**, 2651–2657
  37. Hu, C. H., McStay, B., Jeong, S.-W., and Reeder, R. H. (1994) *Mol. Cell. Biol.* **14**, 2871–2882
  38. Kuhn, A., Voit, R., Stefanovsky, V., Evers, R., Bianchi, M., and Grummt, I. (1994) *EMBO J.* **13**, 416–424
  39. Brady, J. P., Duncan, M. K., Wawrousek, E. F., and Piatigorsky, J. (1997) *Exp. Eye Res.* **64**, 287–290
  40. Omori, Y., Kyushiki, H., Takeda, S., Suzuki, M., Kawai, A., Fujiwara, T., Takahashi, E., and Nakamura, Y. (1997) *Cytogenet. Cell Genet.* **78**, 285–288
  41. Matheny, C., Day, M. L., and Milbrandt, J. (1994) *J. Biol. Chem.* **269**, 8176–8181
  42. Shields, J. M., and Yang, V. W. (1997) *J. Biol. Chem.* **272**, 18504–18507
  43. Maeda, Y., Hisatake, K., Kondo, T., Hanada, K.-i., Song, C.-Z., Nishimura, T., and Muramatsu, M. (1992) *EMBO J.* **11**, 3695–3704
  44. Jantzen, H.-M., Chow, A. M., King, D. S., and Tjian, R. (1992) *Genes Dev.* **6**, 1950–1963
  45. McStay, B., Frazier, M. W., and Reeder, R. H. (1991) *Genes Dev.* **5**, 1957–1968
  46. Imai, H., Fritzler, M. J., Neri, R., Bombardieri, S., Tan, E. M., and Chan, E. K. L. (1994) *Mol. Biol. Rep.* **19**, 115–124
  47. Wyllie, A. H., Beattie, G. J., and Hargreaves, A. D. (1981) *Histochem. J.* **13**, 681–692
  48. Scheer, U., and Rose, K. M. (1984) *Proc. Natl. Acad. Sci. U. S. A.* **81**, 1431–1435
  49. Roussel, P., André, C., Masson, C., Géraud, G., and Hernandez-Verdun, D. (1993) *J. Cell Sci.* **104**, 327–337
  50. Roussel, P., André, C., Comai, L., and Hernandez-Verdun, D. (1996) *J. Cell Biol.* **133**, 235–246
  51. Bell, P., Dabauvalle, M.-C., and Scheer, U. (1992) *J. Cell Biol.* **118**, 1297–1304
  52. Weisenberger, D., Scheer, U., and Benavente, R. (1993) *Eur. J. Cell Biol.* **61**, 189–192
  53. Benavente, R., Rose, K. M., Reimer, G., Hügler-Dörr, B., and Scheer, U. (1987) *J. Cell Biol.* **105**, 1483–1491
  54. Granick, D. (1975) *J. Cell Biol.* **65**, 418–427
  55. Scheer, U., Hügler, B., Hazan, R., and Rose, K. M. (1984) *J. Cell Biol.* **99**, 672–679
  56. Kuhn, A., Stefanovsky, V., and Grummt, I. (1993) *Nucleic Acids Res.* **21**, 2057–2063
  57. le Douarin, B., Nielsen, A. L., Garmier, J.-M., Ichinose, H., Jeanmougin, F., Losson, R., and Chambon, P. (1996) *EMBO J.* **15**, 6701–6715
  58. Perrin, L., Demakova, O., Fanti, L., Kallenbach, S., Saingery, S., Mal'ceva, N. I., Pimpinelli, S., Zhimulev, I., and Pradel, J. (1998) *J. Cell Sci.* **111**, 2753–2761
  59. Payen, E., Verkerk, T., Michalovich, D., Dreyer, S. D., Winterpacht, A., Lee, B., De Zeeuw, C. I., Grosveld, F., and Galjart, N. (1998) *J. Biol. Chem.* **273**, 9099–9109
  60. Saurin, A. J., Borden, K. L. B., Boddy, M. N., and Freemont, P. S. (1996) *Trends Biochem. Sci.* **21**, 208–214
  61. Su, L., Hershberger, R. J., and Weissman, I. L. (1993) *Genes Dev.* **7**, 735–748
  62. Israeli, D., Tessler, E., Haupt, Y., Elkeles, A., Wilder, S., Amson, R., Telesman, A., and Oren, M. (1997) *EMBO J.* **16**, 4384–4392
  63. Arranz, V., Harper, F., Florentin, Y., Puvion, E., Kress, M., and Ernoult-Lange, M. (1997) *Mol. Cell. Biol.* **17**, 2116–2126
  64. Passananti, C., Corbi, N., Paggi, M. G., Russo, M. A., Perez, M., Cotelli, F., Stefanini, M., and Amati, P. (1995) *Cell Growth Differ.* **6**, 1037–1044